Cancer Immunology, Immunotherapy (2019) 68:1133–1141
https://doi.org/10.1007/s00262-019-02348-2

ORIGINAL ARTICLE

Impact of combination immunochemotherapies on progression of 4NQO-induced murine oral squamous cell carcinoma

Sonja Ludwig[1,2] · Chang-Sook Hong[2,3] · Beatrice M. Razzo[2] · Kellsye P. L. Fabian[4] · Manoj Chelvanambi[4] · Stephan Lang[1] · Walter J. Storkus[2,4,5] · Theresa L. Whiteside[2,3,4,6]

Received: 9 November 2018 / Accepted: 20 May 2019 / Published online: 28 May 2019
© Springer-Verlag GmbH Germany, part of Springer Nature 2019

Abstract

Advanced oral squamous cell carcinomas (OSCC) have limited therapeutic options. Although immune therapies are emerging as a potentially effective alternative or adjunct to chemotherapies, the therapeutic efficacy of combination immune chemotherapies has yet to be determined. Using a 4-nitroquinolone-*N*-oxide (4NQO) orthotopic model of OSCC in immunocompetent mice, we evaluated the therapeutic efficacy of single- and combined-agent treatment with a poly-epitope tumor peptide vaccine, cisplatin and/or an $A_{2A}R$ inhibitor, ZM241385. The monotherapies or their combinations resulted in a partial inhibition of tumor growth and, in some cases, a significant but transient upregulation of systemic anti-tumor $CD8^+$ T cell responses. These responses eroded in the face of expanding immunoregulatory cell populations at later stages of tumor progression. Our findings support the need for the further development of combinatorial therapeutic approaches that could more effectively silence dominant immune inhibitory pathways operating in OSCC and provide novel, more beneficial treatment options for this tumor.

Keywords Carcinogenesis · 4NQO model · Oral squamous cell carcinoma · Chemotherapy · Vaccination · $A_{2A}R$ inhibition

Abbreviations

4NQO	4-Nitroquinoline-*N*-oxide
$A_{2A}R$	Adenosine 2A receptor
ADO	Adenosine
ATCC	American Tissue Culture Collection
ATG	Antagonist
BRAF	Proto-oncogene B-RAF
Ep2R	Prostaglandin receptor for PGE_2
EphA2	Ephrin A2
ICIs	Immune checkpoint inhibitors
NS	Not significant
NSD	No significant difference
OSCC	Oral squamous cell carcinoma
PDGFR	Platelet-derived growth factor receptor
PGE_2	Prostaglandin E_2
RT	Room temperature
UPMC	University of Pittsburgh Medical Center
ZM	ZM241385, $A_{2A}R$ antagonist

Electronic supplementary material The online version of this article (https://doi.org/10.1007/s00262-019-02348-2) contains supplementary material, which is available to authorized users.

✉ Theresa L. Whiteside
whitesidetl@upmc.edu

[1] Department of Otorhinolaryngology and Head and Surgery, University Hospital Essen, Essen, Germany

[2] University of Pittsburgh, Medical Center (UPMC), Hillman Cancer Center, Suite 1.32b, 5117 Centre Ave, Pittsburgh, PA 15213, USA

[3] Department of Pathology, University of Pittsburgh School of Medicine, Pittsburgh, PA 15261, USA

[4] Department of Immunology, University of Pittsburgh School of Medicine, Pittsburgh, PA 15261, USA

[5] Department of Dermatology, University of Pittsburgh School of Medicine, Pittsburgh, PA 15261, USA

[6] Department of Otolaryngology, University of Pittsburgh School of Medicine, Pittsburgh, PA 15213, USA

Introduction

Patients with advanced-stage oral squamous cell carcinoma (OSCC) have a poor clinical prognosis due to their common (intrinsic or acquired) resistance to conventional chemoradiotherapies and a highly immunosuppressive tumor microenvironment (TME) favoring disease progression [1, 2]. Five-year survival has remained at < 50% and has not improved for decades, despite numerous advances in surgical as well

as oncological therapies [3]. Immunotherapy, in the form of immune checkpoint inhibitors (ICIs), has recently been introduced as a promising therapeutic option for patients with solid tumors, including OSCC [4–7]. However, only a small minority (< 15%) of patients with advanced-stage head and neck squamous cell carcinoma (HNSCC) have responded to ICIs, such as Nivolumab (anti-PDL1), as reported in a recent phase I clinical trial [8]. Since the majority of HNSCC patients do not respond to monotherapy with ICIs, there is an urgent need to: (a) identify mechanisms underlying tumor resistance to interventional ICIs and (b) define alternate or adjunct immunotherapy strategies that might supersede or synergize with ICIs in the setting of OSCC. Because OSCC is characterized by a highly suppressive TME, it is anticipated that successful immunotherapies against OSCC will need to subvert or eliminate active immunosuppression mechanisms that go beyond those impacted by ICIs.

Numerous regulatory pathways appear to negatively impact protective anti-tumor immune responses in OSCC [4]. Among these, the adenosine (ADO) catabolism and COX-2/PGE_2-synthesis pathways are considered to be dominant contributors to immune dysfunction [9]. OSCC produces and releases large quantities of ADO and PGE_2 into the TME [10, 11]. Both pathways operate via the downregulation of cAMP levels in immune responder cells brought about by ADO ligation of adenosine 2A receptors (A_{2A}Rs) and/or by PGE_2 binding to Ep2Rs on the immune cell surface [12]. The resulting signaling leads to the suppression of effector T cell functions and to the upregulation of immunosuppressive activities mediated by Treg and/or MDSC [13]. Effective antagonism of the ADO- or PGE_2-mediated suppressive pathways is a logical next step in the evolution of cancer immunotherapy designs [9], and several inhibitors of these pathways are currently being evaluated for efficacy in pre-clinical and early-stage clinical trials [14–16].

Another strategy to bolster anti-tumor immunity in OSCC has been the use of therapeutic vaccines targeting tumor-specific T cells. Multiple pre-clinical and clinical vaccination studies have been performed attempting to restore/reinvigorate tumor-specific $CD8^+$ and $CD4^+$ T cells, with variable degrees of success reported [17–19]. We have recently determined that effective therapy of solid tumors in mice and man can be achieved using a syngeneic/autologous DC-based vaccine that targets antigens preferentially expressed by the tumor vasculature [20]. This vaccine overcomes local immune suppression based on its ability to reduce Treg and MDSC content in the TME [21].

With the aim of restricting/limiting tumor-induced immune suppression and enhancing protective immunity against OSCC, we investigated the comparative therapeutic benefits of DC/peptide-based vaccines, cisplatin and an A_{2A}R antagonist, ZM241385, which is currently in clinical trials as a potentially non-toxic addition to chemotherapy [22]. The drugs, delivered as monotherapies or in combination, are tested in the 4NQO-induced murine model of OSCC [23]. This is an immune-competent orthotopic model. Mice treated with 4NQO (a carcinogen) supplied in drinking water first develop pre-malignant lesions which then progress to oral tumors [24]. The tumor developmental pathway in 4NQO mice closely recapitulates that of human OSCC [25]. Here, we report that the monotherapies or their combinations resulted in a partial inhibition of tumor growth which was accompanied by only modest and transient development of tumor-specific immunity. These results are not unexpected, and they indicate that in an immunocompetent mouse model, which closely mimics human OSCC, immune therapies that are effective in other mouse models show only limited therapeutic benefits.

Materials and methods

Mice

A carcinogen, 4-nitroquinoline-*N*-oxide (4-NQO; 100 µg/ml, Sigma Aldrich) was administered to mice *ad libidum* in drinking water for 16 weeks, followed by provision of regular water for the remainder of the experimental period (Supplemental Fig. 1). At the 16-week time point, mice were randomly assigned to different treatment groups (5–7 mice/group): (i) 1. vaccine only, 2. control; (ii) 1. cisplatin only, 2. vaccine only, 3. cisplatin + vaccine, 4. control; (iii) 1. low dose A_{2A}R antagonist, 2. control; (iv) 1. high-dose A2A antagonist, 2. high-dose A2A antagonist + vaccine, 3. control.

Throughout the experiment, mice were continuously monitored for signs of distress and weight loss. Mice were euthanized at the planned conclusion of the experiment (i.e., 28 weeks after the experiment started) or when the weight loss exceeded 20% of the initial body mass. At the time of euthanasia, the tongue and esophagus were harvested and examined for the presence of tumors. The tumor volume was determined by caliper measurements using the formula: length × width × height × π/6 [26].

Tissue preparation and staining

Tissues were processed as described previously [27]. Briefly, tissues were fixed in 4% paraformaldehyde in PBS (Santa Cruz, San Juan, USA) at room temperature (RT) for 2 h and cryopreserved in 30% sucrose overnight (wt/vol in PBS, Sigma Aldrich) for 24 h at 4 °C. All tissues were embedded in Tissue Tek OCT compound (VWR) and frozen in liquid nitrogen. Six-micron cryosections were prepared, stained using a hematoxylin and eosin stain kit (Vector Labs, Cat

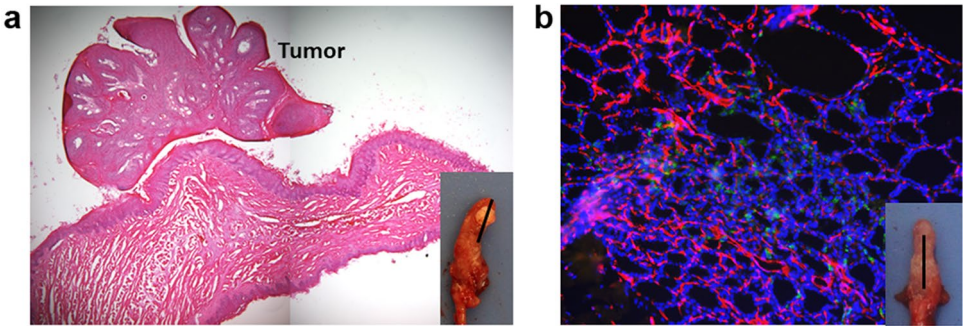

Fig. 1 Histopathology of 4NQO-induced OSCC. OSCC tumor-bearing mice were killed in week 24 and tumors harvested. In **a** H&E staining of a representative tongue tumor. In **b** immunofluorescence staining for Ki67 (green: proliferating cells), DAPI (blue: cell nuclei) and CD31 (red: tumor vasculature) in a representative tongue tumor harvested on day 23. The panel insert indicates the locations of tumors on the tongue

no: H-3502) and evaluated by a pathologist for the presence of OSCCs. Consecutive sections were then stained for CD4 (Alexa Fluor 488, Clone RM4-5, Biolegend Cat no:100529), CD8 (PE, Clone 53-6.7, BD Biosciences Cat no: 553033), FoxP3 (APC, Clone FJK16s, eBioscience Cat no: 17577382), CD31 (PE, Clone MEC 13.3, BD Biosciences, Cat. No: 553373), Ki67 (FITC, Clone SolA15, Thermo Fisher, Cat. No: 11-5698-82), with appropriate isotype controls also tested in separate serial sections. Where indicated, sections were counterstained using DAPI to detect cell nuclei, as previously described [28]. Sections were then covered in Gelvatol (Monsanto, St. Louis, MO) and a coverslip applied. Images of H&E and fluorescently stained sections were acquired on an Olympus Provis Inverted Fluorescence Microscope housed at the Center for Biologic Imaging at the University of Pittsburgh (Pittsburgh, PA). Acquired images were imported to Nikon NIS-Elements for quantification of TIL by the phenotype (CD4+, CD8+, CD4 + FoxP3 + and CD8 + FoxP3 +), vascular content (CD31) and proliferating cells (Ki67).

Therapy groups

Cisplatin Cisplatin (Sigma-Aldrich, PHR1624) was suspended in sterile PBS as per the manufacturer's instructions. Following the initial 16-week 4-NQO treatment, mice randomized to the Cisplatin or Cisplatin + Vaccine treatment groups received a single i.p. injection of Cisplatin at a dose of 2.5 mg/kg. *Vaccine* For vaccine preparation, syngenic DCs were generated from the bone marrow of naïve C57BL/6 mice as previously described [28, 29]. Briefly, bone-marrow cells were cultured in RPMI medium (Life Technologies, Grand Island, NY) supplemented with rmGM-CSF and rmIL-4 (1000 U/ml each, both from Peprotech, Rocky Hill, NJ) for 5 days at 37 °C in 5% CO_2. $CD11c^+$ DC was autoMACS-purified as per the manufacturer's protocol (Miltenyi Biotec, Auburn, CA) and infected with recombinant adenovirus encoding mIL-12p70 for 48 h as previously described [30]. 10^7 harvested DCs were then pulsed with an equimolar mix (1 μM each) of the following known or predicted H-2^b class I-presented synthetic peptide epitopes derived from the murine tumor- or tumor vasculature-associated antigens: $BRAF_{679–687}$ [31], $EGFR_{1131–1139}$, $EphA2_{671–679}$ [32], $EphA2_{682–689}$ [32], $p53_{158–166}$ [33], $p53_{232–240}$ [34], $PDGFR\beta_{539–547}$, $STAT3_{309–316}$, $Survivin_{97–104}$ [35] and $VEGFR2_{615–625}$ [36]. Peptides were synthesized to a purity > 95% by the Hillman Cancer Center's Peptide Synthesis Facility (a shared resource) and analyzed for purity by the Hillman Cancer Center's Protein Sequencing Facility (a shared resource). For vaccination, peptide-loaded DC was briefly washed in PBS and then injected (10^6 DC in a total volume of 50 μl PBS) subcutaneously into the right flank of tumor-bearing mice in weeks 18, 19, 20, 22 and 24.

$A_{2A}R$ antagonist

The $A_{2A}R$ antagonist, ZM241385 (ZM; Tocris Bioscience, Bristol, UK), was prepared as previously described [37]. Briefly, it was dissolved in DMSO, Cremopher (EMD Millipore, Billerica, MA, USA) and ddH_2O at a DMSO:Cremopher:ddH_2O ratio of 1:1:4. Low-dose (0.2 μg ZM/mouse) or high-dose (0.4 μg ZM/mouse) injections were administered i.p. daily to mice, beginning in week 16 of the experiments.

Evaluation of specific $CD8^+$ T cells, MDSC and Treg from treated mice

For the evaluation of vaccine-specific T cell responses from untreated versus treated mice, spleens were harvested from mice harboring median size lesions in weeks 21 and 25 of the experiment, and $CD8^+$ T cells isolated by MACS (Miltenyi) and then analyzed in IFN-γ ELISPOT assays (Mabtech) as previously described [38] using syngenic EL-4

thymoma cells (H-2^b; ATCC) pulsed with individual vaccine peptides (1 μM) as target cells. Untreated EL4 cells served as a negative control, while stimulation with anti-CD3/CD28 antibodies served as a positive control in ELISPOT assays. ELISPOT assays were performed in triplicate wells for each peptide or control. MDSC ($CD11b^+Gr1^+$) and Treg ($CD4^+Foxp3^+$) content in total splenocytes was determined by flow cytometry as previously described [38], using fluorescently labeled antibodies reactive against the following target molecules CD4 (PE/Dazzle 594, Clone OKT4, Biolegend, Cat. no: 317448), CD11b (APC, Clone M1/70, Thermo Fisher, Cat. no: 17-0112-81), FoxP3 (APC, Clone FJK-16 s, ThermoFisher, Cat. no: 17-5773-80) and Gr1 (PE, Clone 1A8, BD Biosciences, Cat. no: 551461). For intracellular staining of FoxP3, the FoxP3/Transcription factor staining buffer set (eBioscience) was implemented.

Statistical analysis

Data were compared and visualized using unpaired *t* test or one-way ANOVA with post hoc analysis. Longitudinal differences in the mice body weights were compared by repeated measures ANOVA using Graph Pad Prism 7 software. *p* values < 0.05 were considered to be statistically significant.

Results

Mechanisms responsible for decreases in tumor progression and induced by monotherapy of 4NQO-induced OSCC with a poly-epitope peptide vaccine

Female C57BL/6 WT mice received 4-NQO (4-nitroquinoline-1-oxide) in drinking water for 16 consecutive weeks and reproducibly (100% take) developed oral tumors. Control mice receiving regular drinking water remained tumor free. The treatment period of 16 weeks was followed by an observation period of several weeks during which mice first developed pre-cancerous lesions (week 21–25) and then cancerous lesions (week 25–29) in the tongue and esophagus. Tumors of variable size were detected on the tongues of mice by weeks 23–24 based on histochemical (H&E) assessments (Fig. 1a). Immunofluorescence analyses of tissue sections revealed an extensive $CD31^+$ blood vessel network and the presence of $Ki67^+$ proliferating cells in the TME (Fig. 1b). Notably, mice receiving 4-NQO displayed only small (NS) reduction of body weight over time after week 16 (control/No therapy mice in Fig. 2a). In this 4-NQO orthotopic model, a loss of body weight may be a consequence of restriction in food uptake and may not directly relate to disease progression.

To determine the potential protective impact of a vaccine designed to elicit therapeutic $CD8^+$ T cells, we treated 4-NQO conditioned mice with syngeneic Type-1-polarized DCs loaded with an equimolar pool of H-$2K^b$- or H-$2D^b$-presented peptide epitopes derived from the tumor (BRAF wt, EGFR, p53, STAT3, Survivin) or tumor vasculature-associated antigens (EphA2, PDGFRβ, VEGFR2). After first determining the optimal frequency for vaccine delivery in preliminary experiments (data not shown), we administered 10^6 pooled peptide-pulsed DC s.c. in the right flank of mice on weeks 18, 19, 20, 22 and 24. This vaccination schedule did not result in the maintenance of higher average body weights in the vaccine cohort vs. the untreated control group (Fig. 2a: $p > 0.05$), although all vaccinated mice appeared healthier (shiny fur) for the duration of the experiment. However, animals treated with the vaccine did not exhibit a significant decrease in tumor burden when compared to control untreated mice (Fig. 2b, $p > 0.05$).

To determine whether active vaccination led to the activation of antigen-specific T cells, treated animals were culled from the vaccine vs. control groups at week 21, and splenic $CD8^+$ T cells were analyzed using IFN-γ ELISPOT assays for their recognition of syngeneic (antigen-presenting) EL-4 thymoma cells pulsed with individual peptides employed in the poly-epitope vaccine (Fig. 2c, d). While T cells isolated from the non-treated control mice failed to recognize any of the vaccine peptides based on IFN-γ secretion (Fig. 2c), $CD8^+$ T cell responses against the $BRAF_{679–687}$, $EphA2_{671–679}$, $EphA_{682–689}$, $Survivin_{97–104}$, $STAT3_{309–316}$ and $VEGFR2_{615–625}$ peptide epitopes were readily observed after specific vaccination (Fig. 2d, $*p < 0.05$, $**p < 0.01$). $CD8^+$ T cell reactivity against the $STAT3_{309–316}$ peptide epitope appeared to be most robust within the poly-specific $CD8^+$ T cell repertoire of the vaccinated animals (Fig. 2d, $****p < 0.0001$). Despite the ability of the vaccine to elicit systemic antigen-specific $CD8^+$ T cell responses in tumor-bearing mice, the immune composition of the TME of vaccinated mice was slightly reduced in $CD4^+$ T cell and $CD8^+$ T cell content, with no significant difference in the ratio of Treg:$CD8^+$ T cells (Fig. 2e, Supplemental Table 1).

During weeks 21 and 25 of the experiment, splenocytes harvested from animals in the control versus vaccine cohorts were also evaluated for their levels of immunoregulatory cell populations, including Treg and MDSC (Supplemental Fig. 2). We observed that while the frequency of $CD4^+Foxp3^+$ Treg was not impacted by therapeutic intervention at either time point, the frequency of $CD11b^+Gr1^+$ MDSC declined ($p < 0.05$) in the vaccinated mice on week 21 (Supplemental Fig. 2). However, this reduction in MDSC was completely eroded by week 25, with nearly half of all myeloid cells in the spleen exhibiting an MDSC phenotype regardless of prior treatment. These experiments indicated that the poly-epitope vaccine

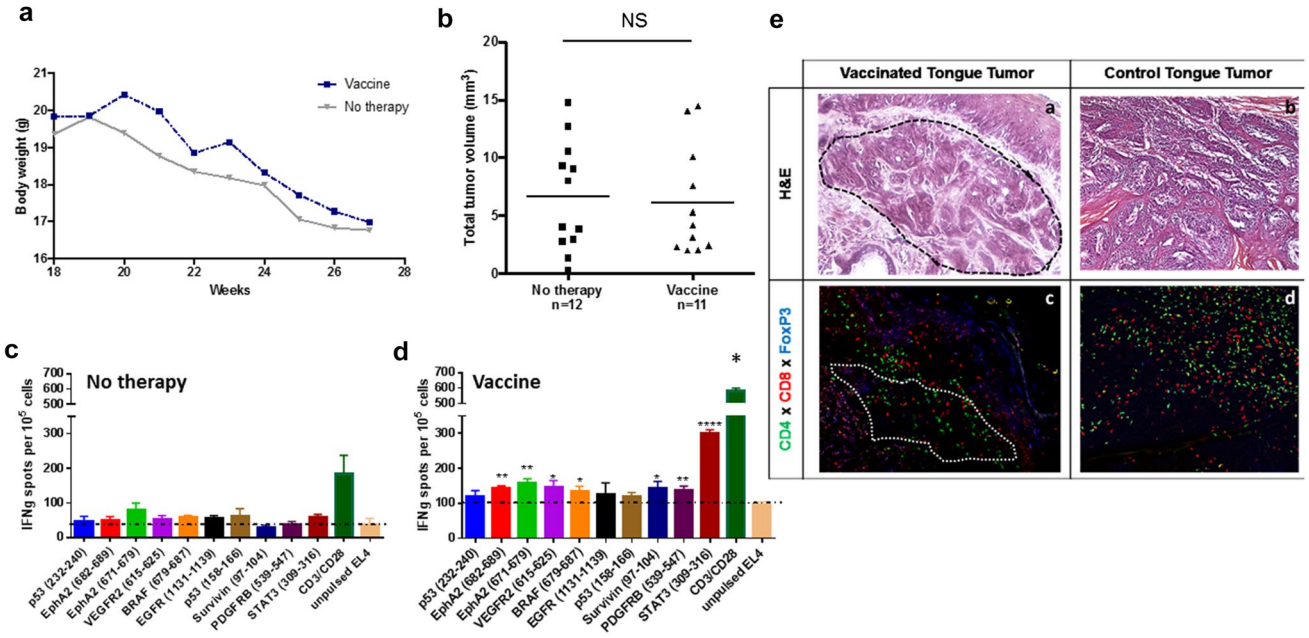

Fig. 2 Treatment of OSCC tumor-bearing mice with a poly-peptide vaccine results in the induction of specific $CD8^+$ T cells but fails to impact disease progression. Mice bearing 16 week pre-malignant lesions were treated s.c. with a poly-epitope vaccine on weeks 18, 19, 20, 22 and 24. In **a** the average body weights of the vaccine-treated mice did not change vs. those of untreated control mice from week 19 onward ($p > 0.05$). In **b,** total tumor volumes (tongue and esophageal tumors) were equal in the vaccinated vs. control mice ($p > 0.05$). In **c**, **d** IFN-γ ELISPOT data are shown for splenic $CD8^+$ T cells isolated from control (**c**) or vaccinated (**d**) mice after stimulation with EL4 thymoma cells presenting individual vaccine peptides or anti-CD3/anti-CD28 (positive control). The presented data are from one of the two independent experiments; $^*p < 0.05$, $^{**}p < 0.01$, $^{****}p < 0.0001$. In **e** OSCC tumors from vaccinated vs. control untreated mice were H&E stained [upper panels; tumor is marked by dotted boundary] Lower panels show results of fluorescence imaging of immune cell infiltrates using directly labeled antibody probes for CD4, CD8 and FoxP3. Quantitation of the **e** fluorescence images is reported in Supplemental Table 1

failed to provide extended therapeutic benefits to mice bearing established 4NQO tumors, most likely due to the overwhelming influence of regulatory immune cell populations (Treg, MDSC).

Monotherapy with cisplatin reduces tumor load but not the loss of body weight

We next investigated whether treatment of mice with cisplatin inhibited disease progression and to what extent when compared with the poly-epitope vaccine. As shown in Fig. 3a, although monotherapy with cisplatin did not result in a significant improvement in body weight, it was associated with a reduction in total tumor load (Fig. 3b, $p < 0.05$). Interestingly, treatment with cisplatin only impacted the volume of 4NQO-induced tumors in the tongue but not the esophagus (Fig. 3c, d). When comparing the monotherapies consisting of poly-epitope vaccine vs. cisplatin head-to-head, cisplatin exhibited greater salutary effects on tumor progression, while the vaccine failed to significantly impact body mass or tumor load (Fig. 3, $p > 0.05$).

Monotherapy with the $A_{2A}R$ antagonist, ZM241385, decreases tumor volume, activates $CD8^+$ T cells and reduces the frequency of splenic MDSC

Two cohorts of mice conditioned for 16 weeks with 4NQO were treated with either low-dose (0.2 µg/mouse) or high-dose (0.4 µg/mouse) ZM241385. Treatment with low-dose ZM241385 did not preserve body weight (Fig. 4a, NS), while limiting progression of disease in the tongue (but not the esophagus), with minimal impact on total tumor volume (Fig. 4b–d). Higher dosing with ZM241385 also did not preserve average body weight (Fig. 4e, NS), but it promoted a reduction in total tumor volume (including the tongue and the esophagus) when compared to the control group (Fig. 4f–h, $^*p < 0.05$ or $^{**}p < 0.01$). Furthermore, at the higher dose, ZM242385 increased the frequency of splenic $CD8^+$ T cells responding in the IFN-γ ELISPOT assay against the p53 and VEGFR2 peptide epitopes, although this degree of enhancement failed to reach significance (Fig. 5f; $p > 0.05$). Therapy with the higher dose of ZM241385 also led to a decrease in the frequency of MDSC (but not Treg) in the spleen (Supplemental Fig. 3).

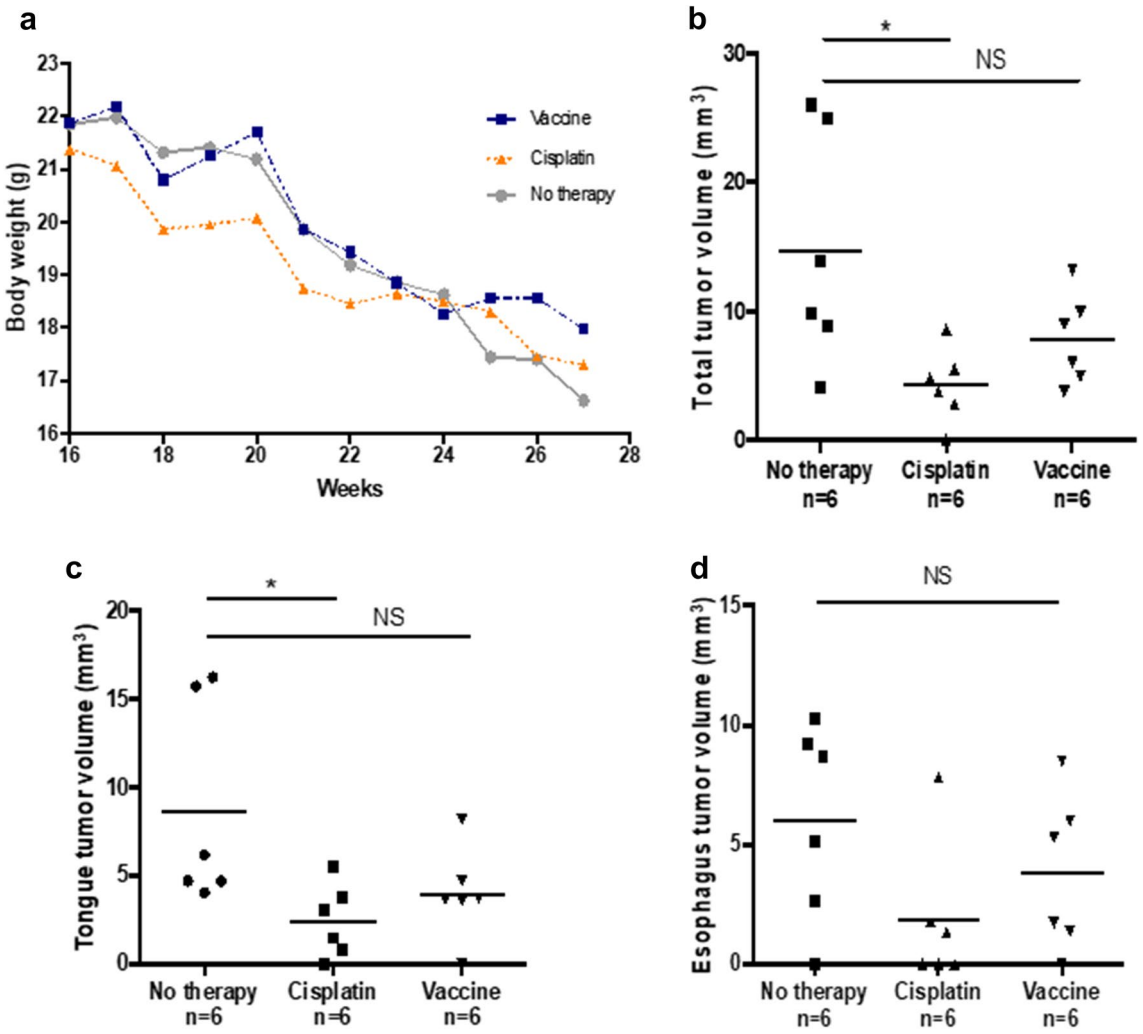

Fig. 3 Modest, but superior impact of treating OSCC tumor-bearing mice with cisplatin vs. poly-peptide vaccine monotherapy. In **a,** the average body weight of mice treated with cisplatin did not change relative to that in untreated mice, and it was not statistically different vs. mice treated with the vaccine ($p > 0.05$). Treatment with cisplatin but not vaccine was associated with significantly reduced total tumor volume (**b**) and the tongue tumor volume (**c**), but not the esophageal tumor volume (**d**) versus control untreated mice. *NS* not significant; $^{*}p > 0.05$

Lack of therapeutic benefit for combinatorial therapy with high-dose $A_{2a}R$ ATG plus vaccine

Combination treatment of OSCC-bearing mice with the poly-epitope vaccine plus high-dose ZM241385 failed to provide statistically superior maintenance of body weight over time (Fig. 5a; NS) or to control tumor volume (Fig. 5b; NS) when compared to control untreated animals. Combining the poly-epitope vaccine with high-dose A2A ATG treatment did, however, mildly up-regulate $CD8^{+}$ T cell functionality in ELISPOT assays (data not shown) and decrease the frequency of MDSC (but not Treg) in the spleen (Supplemental Fig. 3).

Moderate therapeutic effects of combinational therapy with cisplatin plus vaccine

The combination of cisplatin and the poly-epitope vaccine did not lead to significant recovery of body weight over time compared to the control group (Supplemental Fig. 4a; NS) but it did significantly reduce total tumor volume and esophageal tumor volume (Supplemental Fig. 4b, d; $^{*}p < 0.05$).

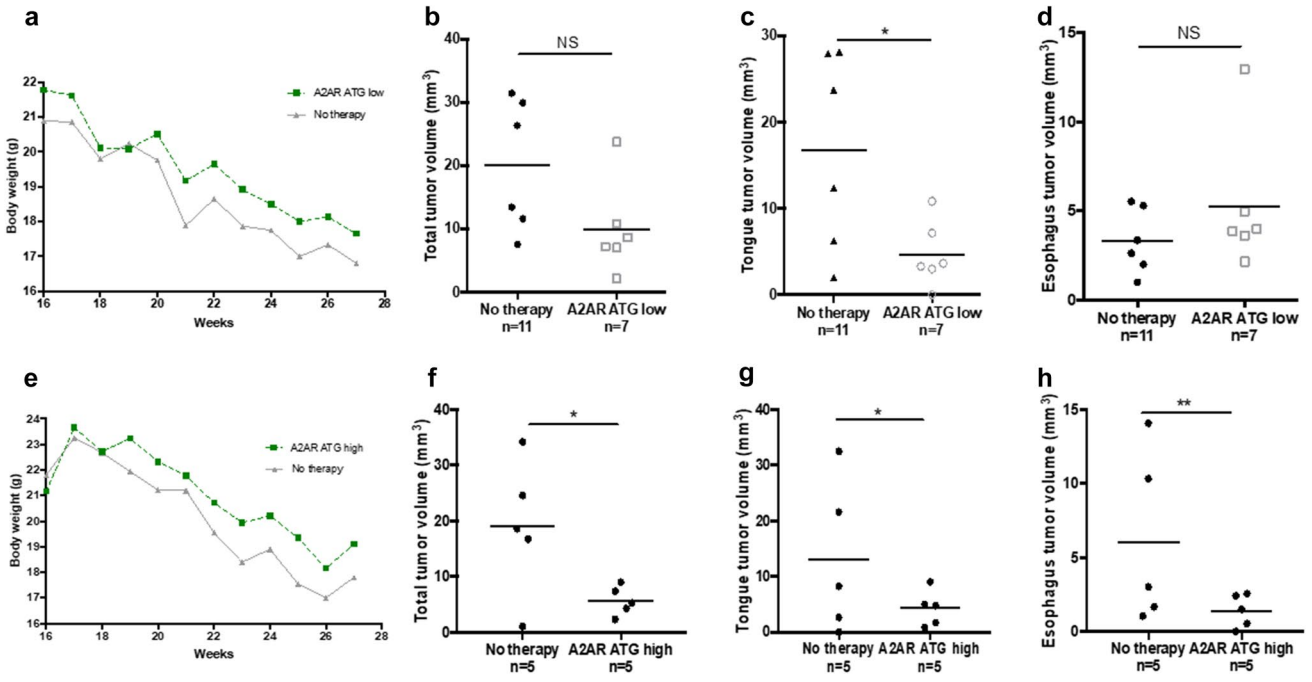

Fig. 4 Modest but superior impact of monotherapy with high- vs. low-dose $A_{2A}R$ antagonist ZM241385 on OSCC tumor growth. OSCC-bearing mice received therapy consisting of low- (0.2 µg/mouse; **a**) or high- (0.4 µg/mouse; **e**) dose $A_{2A}R$ antagonist did not change the average body weight vs. untreated control mice ($A_{2A}R$ low: NS; $A_{2A}R$ high: NS). In **b**–**d**, **f**–**h** only therapy with high-dose $A_{2A}R$ antagonist lead to significant inhibition of the total tumor volume of both tongue and esophageal tumors; $*p<0.05$, $**p<0.01$

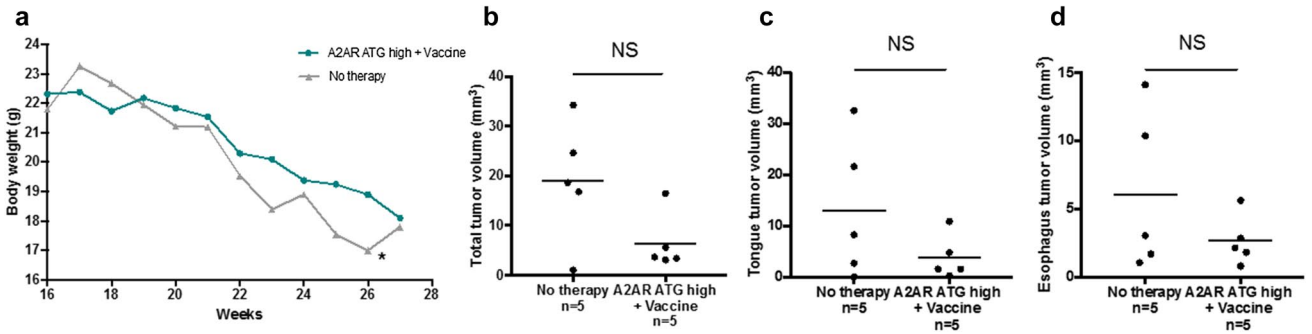

Fig. 5 Minimal therapeutic impact for combination treatment using poly-peptide vaccination plus high-dose $A_{2A}R$ antagonist (ATG). In **a,** changes over time in average body weights are compared for mice receiving the combined therapy vs. untreated controls ($p<0.01$ for week 26 only; indicated by an asterisk; NS for other time points). In **b**–**d** while the tumor volumes appear to be smaller in mice receiving the combined therapy vs. control untreated mice, these differences failed to reach significance (NS for all)

Discussion

Traditional therapeutic modalities have yielded only modest clinical benefits and/or unacceptable toxicities in the setting of advanced-stage OSCC. The identification of novel, more effective intervention strategies remains a major unmet clinical need [4]. Over the past decade, immunotherapies, including administration of ICIs, have provided promising results in patients with advanced/metastatic HNSCC [8], supporting a paradigm for treatment-induced restoration of anti-tumor immune function capable of mediating disease resolution. However, overwhelming immune suppression in the TME of OSCC driven by suppressor cells (Treg, MDSC), suppressive factors produced by the tumor, inhibitory receptor/ligand interactions and tumor-derived extracellular vesicles (EVs) [39] provides a broad range of therapeutic targets that may be difficult to address in simplistic therapy designs. In view of this overwhelming immunosuppressive landscape of OSCC, more effective strategies able to coordinately block a range of inhibitory pathways operational

within the TME are necessary. At the same time, these strategies must support protective anti-tumor effector cell viability and functions. This approach to overcoming tumor-induced immune suppression has been previously discussed in the literature [40–46].

The current studies were performed to assess the anti-tumor impact of single- and combined-agent therapies (vaccines, cisplatin, $A_{2A}R$ antagonist) on the growth of 4NQO carcinogen-induced OSCC in mice. Our study differs from other in vivo reports on OSCC immunotherapy [47, 48]. We have used an orthotopic mouse tumor model that is immunocompetent and that closely approximates the development and histological as well as immunological features of human OSCC. Thus, the TME of 4NQO mice appears to be comparable to its human counterpart [23]. Further, the model affords the benefit of delivering therapeutic intervention at the early/pre-malignant stage when lesions are more responsive to therapy than well-established tumors. The advantages offered by the 4NQO model are counterbalanced by the extended time span needed for the tumor development, although this again is reminiscent of the development of human OSCC.

Somewhat disappointingly, the monotherapies that we investigated in 4NQO models yielded only modest anti-tumor benefits that were transient in nature. A comparison of the poly-epitope vaccine, cisplatin and $A_{2A}R$ antagonist ZM241385 monotherapies did not identify a therapy that had superior therapeutic effects. The poly-epitope vaccine was competent in promoting activation of antigen-specific $CD8^+$ T effector cells (in the spleen), but these T cells appeared to be insufficient in numbers or functional activity to overcome the immunosuppressive effects of the TME in our OSCC model. Only treatment with high-dose ZM241385 led to a significant, but transient, reduction in tumor load. This result was not unexpected, as the adenosine axis is recognized as a major suppressive mechanism in OSCC [49] and is being targeted in ongoing phase I clinical trials for head and neck cancer [16]. The results of this study serve to remind us that in advanced or progressing disease, immune therapies might lead to transient "rejuvenation" of anti-tumor immunity; however, in the presence of overwhelming tumor-induced immune dysfunction, this rejuvenation is unlikely to result in effective therapeutic responses to monotherapy or even combinatorial therapies.

Surprisingly, combined treatment of OSCC-bearing mice with the poly-epitope vaccine + ZM241385 was not therapeutically superior to monotherapy with either component. It is possible that further optimization of the administered drug concentrations or further modification of the schedule for delivery of the drug would provide superior anti-tumor activity in vivo. For example, future studies could test the vaccine in combination with reagents known to target Treg/MDSC prevalence (i.e., low-dose cyclophosphamide/Ontak/anti-Gr-1). Nevertheless, given the perception that tumor-induced immunosuppressive mechanisms are numerous, varied and likely to be highly active in progressing tumors, combination chemoimmunotherapies will invariably emerge as preferred future treatment options for patients with OSCC. With this in mind, the 4NQO model should be considered as a relevant platform for the pre-clinical evaluations of prospective therapy designs.

Author contributions SoL designed and performed all experiments and wrote the manuscript. C-SH assisted with all in vivo experiments. BMR helped with generating 4NQO mice. KPLF and MC performed IHC, IF, ELISPOT assays. StL provided financial support for the project. WJS supervised and interpreted in vivo experiments. TLW supervised all experiments, interpreted results and edited the manuscript.

Funding This project used the UPMC Hillman Cancer Center Peptide Synthesis Core Facility supported in part by NIH P30 CA047904. This work was also supported by NIH R01 CA168628 (Theresa L. Whiteside). Sonja Ludwig was supported by the Pittsburgh-Essen Partnership Program (iFORES) of the University Duisburg-Essen, Essen, Germany.
Compliance with ethical standards

Compliance with ethical standards

Conflict of interest The authors declare that they have no conflicts of interest.

Ethical approval All animal experiments were performed in accordance with the guidelines of the Institutional Animal Care and Use Committee (IACUC) at the University of Pittsburgh and the Hillman Cancer Center (IACUC protocol # 16088780).

Animal source Female 6-week-old C57BL/6 WT mice were purchased from The Jackson Laboratory, Bar Harbor, ME, USA and were housed under pathogen-free conditions.

Cell line authentication No cell lines were used. DC.IL-12 cells are murine DCs isolated from the bone marrow, cultured and infected with recombinant adenovirus encoding mIL-12p70.

References

1. Eckert AW et al (2016) Clinical relevance of the tumor microenvironment and immune escape of oral squamous cell carcinoma. J Transl Med 14:85
2. Leemans CR, Braakhuis BJ, Brakenhoff RH (2011) The molecular biology of head and neck cancer. Nat Rev Cancer 11(1):9–22
3. Ferlay J et al (2015) Cancer incidence and mortality worldwide: sources, methods and major patterns in GLOBOCAN 2012. Int J Cancer 136(5):E359–E386
4. Whiteside TL (2018) Head and neck carcinoma immunotherapy: facts and hopes. Clin Cancer Res 24(1):6–13
5. Melero I et al (2018) Introducing a new series: immunotherapy facts and hopes. Clin Cancer Res 24(8):1773–1774
6. Economopoulou P et al (2016) The promise of immunotherapy in head and neck squamous cell carcinoma. Ann Oncol 27(9):1675–1685

7. Cekic C et al (2014) Myeloid expression of adenosine A2A receptor suppresses T and NK cell responses in the solid tumor microenvironment. Cancer Res 74(24):7250–7259
8. Ferris RL et al (2016) Nivolumab for recurrent squamous-cell carcinoma of the head and neck. N Engl J Med 375(19):1856–1867
9. Mandapathil M et al (2010) Adenosine and prostaglandin E2 cooperate in the suppression of immune responses mediated by adaptive regulatory T cells. J Biol Chem 285(36):27571–27580
10. Di Virgilio F, Adinolfi E (2017) Extracellular purines, purinergic receptors and tumor growth. Oncogene 36(3):293–303
11. Mediavilla-Varela M et al (2017) A novel antagonist of the immune checkpoint protein adenosine A2a receptor restores tumor-infiltrating lymphocyte activity in the context of the tumor microenvironment. Neoplasia 19(7):530–536
12. Goetzl EJ, An S, Zeng L (1995) Specific suppression by prostaglandin E2 of activation-induced apoptosis of human CD4+CD8+ T lymphoblasts. J Immunol 154(3):1041–1047
13. Whiteside TL (2015) The role of regulatory T cells in cancer immunology. Immunotargets Ther 4:159–171
14. Leone RD, Emens LA (2018) Targeting adenosine for cancer immunotherapy. J Immunother Cancer 6(1):57
15. Hutchinson L (2015) Immunotherapy: evading immune escape: synergy of COX and immune-checkpoint inhibitors. Nat Rev Clin Oncol 12(11):622
16. Beavis PA et al (2015) Adenosine receptor 2A blockade increases the efficacy of anti-PD-1 through enhanced antitumor T-cell responses. Cancer Immunol Res 3(5):506–517
17. Durgeau A et al (2018) Recent advances in targeting CD8 T-cell immunity for more effective cancer immunotherapy. Front Immunol 9:14
18. Zhou G, Drake CG, Levitsky HI (2006) Amplification of tumor-specific regulatory T cells following therapeutic cancer vaccines. Blood 107(2):628–636
19. Mould RC et al (2017) Enhancing immune responses to cancer vaccines using multi-site injections. Sci Rep 7(1):8322
20. Liu Z et al (2017) Intratumoral delivery of tumor antigen-loaded DC and tumor-primed CD4(+) T cells combined with agonist alpha-GITR mAb promotes durable CD8(+) T-cell-dependent antitumor immunity. Oncoimmunology 6(6):e1315487
21. Arab S et al (2017) Increased efficacy of a dendritic cell-based therapeutic cancer vaccine with adenosine receptor antagonist and CD73 inhibitor. Tumour Biol 39(3):1010428317695021
22. Leone RD, Lo YC, Powell JD (2015) A2aR antagonists: next generation checkpoint blockade for cancer immunotherapy. Comput Struct Biotechnol J 13:265–272
23. Hawkins BL et al (1994) 4NQO carcinogenesis: a mouse model of oral cavity squamous cell carcinoma. Head Neck 16(5):424–432
24. Schoop RA, Noteborn MH, BaatenburgdeJong RJ (2009) A mouse model for oral squamous cell carcinoma. J Mol Histol 40(3):177–181
25. Yang Z et al (2013) Comparable molecular alterations in 4-nitroquinoline 1-oxide-induced oral and esophageal cancer in mice and in human esophageal cancer, associated with poor prognosis of patients. Vivo 27(4):473–484
26. Tomayko MM, Reynolds CP (1989) Determination of subcutaneous tumor size in athymic (nude) mice. Cancer Chemother Pharmacol 24(3):148–154
27. Qu Y et al (2010) Intralesional delivery of dendritic cells engineered to express T-bet promotes protective type 1 immunity and the normalization of the tumor microenvironment. J Immunol 185(5):2895–2902
28. Komita H et al (2008) CD8 + T-cell responses against hemoglobin-beta prevent solid tumor growth. Cancer Res 68(19):8076–8084
29. Son YI et al (2002) A novel bulk-culture method for generating mature dendritic cells from mouse bone marrow cells. J Immunol Methods 262(1–2):145–157
30. Zhao X et al (2012) Vaccines targeting tumor blood vessel antigens promote CD8(+) T cell-dependent tumor eradication or dormancy in HLA-A2 transgenic mice. J Immunol 188(4):1782–1788
31. Liu Q et al (2018) BRAF peptide vaccine facilitates therapy of murine BRAF-mutant melanoma. Cancer Immunol Immunother 67(2):299–310
32. Hatano M et al (2004) Vaccination with EphA2-derived T cell-epitopes promotes immunity against both EphA2-expressing and EphA2-negative tumors. J Transl Med 2(1):40
33. Umano Y et al (2001) Generation of cytotoxic T cell responses to an HLA-A24 restricted epitope peptide derived from wild-type p53. Br J Cancer 84(8):1052–1057
34. Lacabanne V et al (1996) A wild-type p53 cytotoxic T cell epitope is presented by mouse hepatocarcinoma cells. Eur J Immunol 26(11):2635–2639
35. Hofmann UB et al (2009) Identification and characterization of survivin-derived H-2Kb-restricted CTL epitopes. Eur J Immunol 39(5):1419–1424
36. Dong Y et al (2006) Identification of H-2Db-specific CD8 + T-cell epitopes from mouse VEGFR2 that can inhibit angiogenesis and tumor growth. J Immunother 29(1):32–40
37. Waickman AT et al (2012) Enhancement of tumor immunotherapy by deletion of the A2A adenosine receptor. Cancer Immunol Immunother 61(6):917–926
38. Fabian KP et al (2017) Therapeutic efficacy of combined vaccination against tumor pericyte-associated antigens DLK1 and DLK2 in mice. Oncoimmunology 6(3):e1290035
39. Theodoraki MN et al (2018) Clinical significance of PD-L1(+) exosomes in plasma of head and neck cancer patients. Clin Cancer Res 24(4):896–905
40. Chen WC et al (2017) Inflammation-induced myeloid-derived suppressor cells associated with squamous cell carcinoma of the head and neck. Head Neck 39(2):347–355
41. Chu M et al (2012) Myeloid-derived suppressor cells contribute to oral cancer progression in 4NQO-treated mice. Oral Dis 18(1):67–73
42. Fuse H et al (2016) Enhanced expression of PD-L1 in oral squamous cell carcinoma-derived CD11b(+)Gr-1(+) cells and its contribution to immunosuppressive activity. Oral Oncol 59:20–29
43. Schaefer C et al (2005) Characteristics of CD4 + CD25 + regulatory T cells in the peripheral circulation of patients with head and neck cancer. Br J Cancer 92(5):913–920
44. Mandapathil M et al (2009) Increased ectonucleotidase expression and activity in regulatory T cells of patients with head and neck cancer. Clin Cancer Res 15(20):6348–6357
45. Jie HB et al (2013) Intratumoral regulatory T cells upregulate immunosuppressive molecules in head and neck cancer patients. Br J Cancer 109(10):2629–2635
46. Theodoraki MN, Hoffmann TK, Whiteside TL (2018) Separation of plasma-derived exosomes into CD3((+)) and CD3((−)) fractions allows for association of immune cell and tumour cell markers with disease activity in HNSCC patients. Clin Exp Immunol 192(3):271–283
47. Liu JF et al (2018) Inhibition of JAK2/STAT3 reduces tumor-induced angiogenesis and myeloid-derived suppressor cells in head and neck cancer. Mol Carcinog 57(3):429–439
48. Wang L et al (2013) Graft-versus-host disease is enhanced by selective CD73 blockade in mice. PLoS One 8(3):e58397
49. Schuler PJ et al (2014) Human CD4 + CD39 + regulatory T cells produce adenosine upon co-expression of surface CD73 or contact with CD73 + exosomes or CD73 + cells. Clin Exp Immunol 177(2):531–543

Publisher's Note Springer Nature remains neutral with regard to jurisdictional claims in published maps and institutional affiliations.